Osteoarthritis and Cartilage 27 (2019) 1152–1162

Osteoarthritis and Cartilage

Cartilage wear patterns in severe osteoarthritis of the trapeziometacarpal joint: a quantitative analysis

S. Miyamura †, K. Oka †, T. Sakai ‡, H. Tanaka †, R. Shiode †, S. Shimada §, T. Mae †, K. Sugamoto ||, H. Yoshikawa †, T. Murase † *

† *Department of Orthopaedic Surgery, Osaka University, Graduate School of Medicine, 2-2 Yamada-oka, Suita, Osaka 565-0871, Japan*
‡ *Department of Orthopaedic Surgery, Yamaguchi University, Graduate School of Medicine, 1-1-1, Minamikogushi, Ube 755-8505, Japan*
§ *Department of Neuroscience and Cell Biology, Osaka University, Graduate School of Medicine, 2-2 Yamada-oka, Suita, Osaka 565-0871, Japan*
|| *Department of Orthopaedic Biomaterial Science, Osaka University, Graduate School of Medicine, 2-2 Yamada-oka, Suita, Osaka 565-0871, Japan*

ARTICLE INFO

Article history:
Received 18 December 2018
Accepted 27 March 2019

Keywords:
Cartilage wear
First metacarpal
Laser scanner
Osteoarthritis
Trapeziometacarpal joint
Trapezium

SUMMARY

Objective: The present quantitative study aimed to assess the three-dimensional (3-D) cartilage wear patterns of the first metacarpal and trapezium in the advanced stage of osteoarthritis (OA) and compare cartilage measurements with radiographic severity.
Design: Using 19 cadaveric trapeziometacarpal (TMC) joints, 3-D cartilage surface models of the first metacarpal and trapezium were created with a laser scanner, and 3-D bone surface model counterparts were similarly created after dissolving the cartilage. These two models were superimposed, and the interval distance on the articular surface as the cartilage thickness was measured. All measurements were obtained in categorized anatomic regions on the articular surface of the respective bone, and we analyzed the 3-D wear patterns on the entire cartilage surface. Furthermore, we compared measurements of cartilage thickness with radiographic OA severity according to the Eaton grading system using Pearson correlation coefficients (r).
Results: In the first metacarpal, the cartilage thickness declined volarly (the mean cartilage thickness of the volar region was 0.32 ± 0.16 mm, whereas that of the dorsal region was 0.53 ± 0.18 mm). Conversely, the cartilage evenly degenerated throughout the articular surface of the trapezium. Measurements of the categorized regions where cartilage thinning was remarkable exhibited statistical correlations with radiographic staging ($r = -0.48$ to -0.72).
Conclusions: Our findings indicate that cartilage wear patterns differ between the first metacarpal and trapezium in the late stage of OA. There is a need for further studies on cartilage degeneration leading to symptomatic OA in the TMC joint.

Introduction

Among the elderly, the trapeziometacarpal (TMC) joint at the base of the thumb is a common site for symptomatic and radiographic osteoarthritis (OA)[1]. With aging, arthritis of the TMC joint progressively increases in prevalence, and a 91% prevalence has been reported in patients aged > 80 years[2]. Joint degeneration, concomitant with the progress of OA, results in the reduction of joint mobility, exacerbation of pain and swelling, weakness of grip and pinch, and overall disablement of the hand[3,4]. Reportedly, the pathophysiology of this disease is characterized by damage to the articular cartilage, osteophyte formation, changes in the subchondral bone, and synovitis[5], and of these, the articular cartilage has garnered the most attention in relation to its pathogenesis, mainly because of its striking changes in advanced OA[6]. Cartilage wear, which is identified as the narrowing of the joint space on plain radiographs, can cause contact among bones that have many nociceptive fibers, highlighting the contribution to the pain profile[7].

* Address correspondence and reprint requests to: T. Murase, Department of Orthopaedic Surgery, Osaka University, Graduate School of Medicine, 2-2 Yamada-oka, Suita, Osaka 565-0871, Japan. Tel.: 81-6-6879-3552; Fax: 81-6-6879-3559.
E-mail addresses: m1ttyd2s@gmail.com (S. Miyamura), oka-kunihiro@umin.ac.jp (K. Oka), tsakai-osk@umin.ac.jp (T. Sakai), tanahiro-osk@umin.ac.jp (H. Tanaka), frontier.of.mode@gmail.com (R. Shiode), shimada@anat1.med.osaka-u.ac.jp (S. Shimada), ta-mae@umin.ac.jp (T. Mae), sugamoto@ort.med.osaka-u.ac.jp (K. Sugamoto), yhideki@ort.med.osaka-u.ac.jp (H. Yoshikawa), tmurase-osk@umin.ac.jp (T. Murase).

https://doi.org/10.1016/j.joca.2019.03.006
1063-4584/

Furthermore, morphological changes in cartilage have been reported to be associated with disease severity or disease progression in OA[8].

Despite a close correlation between cartilage wear and disease progression, cartilage wear patterns in TMC joint OA remain unclear. The number of studies focusing on the spatial quantification of the articular cartilage of the TMC joint is limited because of the lack of accuracy in detecting the cartilage region on imaging analysis, as well as the morphological complexity of the thin cartilage. In particular, only few objective measures have been documented in advanced-stage OA[4,9,10], although ascertaining the articular cartilage wear pattern in late-stage OA is essential for elucidating the etiology.

Quantification of the three-dimensional (3-D) cartilage thickness distribution in TMC joints with advanced OA could help in the elucidation of how regional variations in the cartilage wear pattern contribute to the etiology of TMC arthrosis, which is a normal part of human aging. Hence, the present study aimed to investigate the 3-D cartilage wear patterns of the first metacarpal and trapezium in advanced-stage OA and compare cartilage measurements with radiographic severity.

Method

Specimens

We harvested 20 wrists from 10 cadavers embedded in formalin. Subjects were eligible for inclusion in this study if they exhibited a radiographic degenerative change in the TMC joint. First, we scanned all specimens with a helical-type CT scanner (Aquilion ONE; Toshiba Medical Systems, Tokyo, Japan), using the following standardized protocol: slice thickness, 0.65 mm; pixel size, 0.75–0.85 mm; scan time, 0.5 s; scan pitch, 0.562:1; tube current, 30 mA; and tube voltage, 120 kV. Subsequently, we selected specimens that had signs of OA in the TMC joint. Of note, one specimen was excluded because of previous wrist surgery (four-corner fusion arthrodesis). Thus, we investigated the remaining 19 wrists harvested from seven male and three female cadavers without anthropometric data, and the left and right wrists were separately analyzed owing to differences in the prevalence of TMC OA[11,12]. The subjects were aged 74–102 (mean age, 89.5) years at the time of death. The study protocol was approved by the Institutional Review Board of our institution. Furthermore, all procedures performed were in accordance with the ethical standards of the responsible committees on human experimentation (institutional and national) and with the Helsinki Declaration of 1975, as revised in 2000.

Cartilage + bone model reconstruction

All specimens were dissected to expose the articular surface of both the first metacarpal and trapezium without damaging the cartilage. The soft tissues, including the skin, muscles, ligaments, and joint capsule, and the structures of the wrist joint were carefully removed. Next, using a 3-D optical laser scanner (accuracy, ± 20 μm; Rexcan CS+ 5.0 M; Medit Company, Seoul, Republic of Korea), we obtained a profile of the TMC joint dimensions. Then, a high-precision, two-axes turntable positioner automatically rotated and swung at defined intervals to capture multiple scans of the object, and points to configure 3-D surface geometry were sampled every 97 μm. The points created triangular meshes (polygon data), and the 3-D models comprised these meshes. Subsequently, we firmly mounted the specimens on a clay base attached to the turntable. For capturing the overall surface of the bones with cartilage, 72 separate scans were required (36 scans at the front and back sides; 12 scans per 30° rotation at 0°, 30°, and −30° swings), ensuring sufficient overlap of adjacent scans. All scans were processed using ezScan7 software (Medit Company, Seoul, Republic of Korea), and 3-D bone models with cartilage were created (cartilage + bone model; Fig. 1).

Bone model reconstruction

We used the cartilage dissolution technique to create 3-D bone models without cartilage to obtain ground truth for the measurement of the articular cartilage[10,13–17]. To dissolve the articular cartilage of the TMC joint, the articular surface of the first metacarpal base and saddle-shaped articular surface of the trapezium were soaked in 6.0% sodium hypochlorite solution for 2–4 h. We visually inspected and checked the cartilage by rubbing with a surgical probe to confirm its complete dissolution. Next, the specimens with cartilage-free articular surfaces were rescanned using the same procedure as that for the cartilage + bone model, and 3-D bone models without cartilage were created (bone model; Fig. 1).

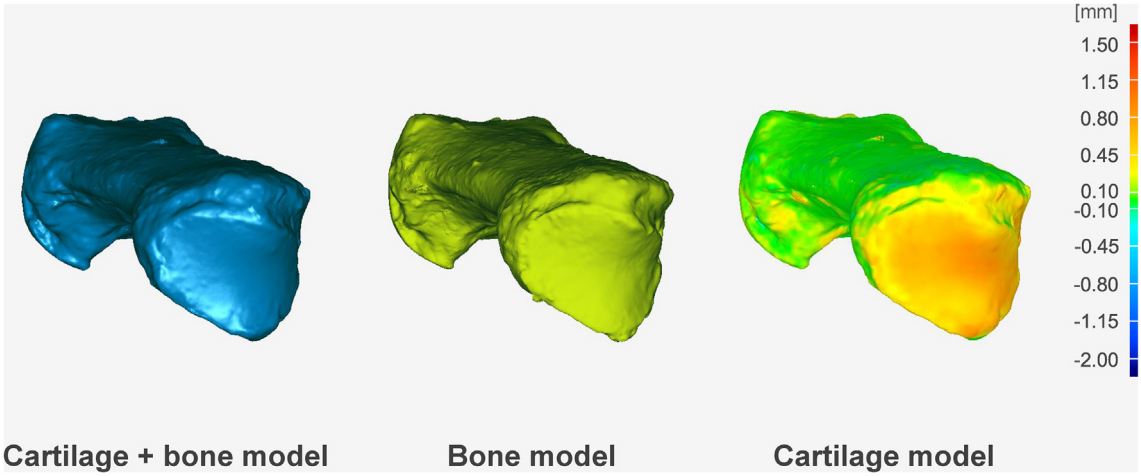

Fig. 1. Images of our three-dimensional (3-D) models: cartilage + bone model (left); bone model (middle); and cartilage model (right). The cartilage model helped in encoding the cartilage thickness information as a thickness map.

Cartilage model creation

The mean numbers of polygon data points of the cartilage + bone and bone models were 957,184 ± 137,806 and 936,950 ± 128,700 for the first metacarpal and 522,655 ± 106,762 and 505,354 ± 99,507 for the trapezium, respectively. These surface model datasets obtained using a 3-D laser scanner were processed with Geomagic Control software (3D Systems, South Carolina, USA) in the STL file format. To create 3-D cartilage models, the bone models were superimposed onto the cartilage + bone models using the iterative closest point algorithm[18], encoding the thickness information of the cartilage + bone model as a thickness map (Fig. 1). With this algorithm, the two models were superimposed using corresponding regions other than the articular cartilage surface to decrease the odds of superimposition error.

Regions of interest

We imported the STL data of the cartilage + bone models into a commercially available software (Bone Simulator; Orthree, Osaka, Japan) to define the regions of interest (ROIs). On the articular surfaces of the first metacarpal and trapezium, the ROIs were set on the basis of anatomical landmarks identified on the 3-D models and saved in the STL file format. Before the measurements, preliminary analyses were conducted for the gross distribution of the cartilage thickness using a statistical method. It was found that the cartilage of the first metacarpal and trapezium was evenly distributed on the articular surface in the radial-to-ulnar direction, whereas the cartilage thickness of the first metacarpal decreased volarly (Supplementary Information). We therefore decided to investigate the trend in the dorsal-to-volar direction in detail. Of note, all definitions and measurements involved the right TMC joint by mirroring the left side.

In the first metacarpal, we used an orthogonal coordinate system based on the International Society of Biomechanics (ISB) recommendation[19]. The *Y*-axis was defined as the principal axis of inertia of the first metacarpal and was automatically computed. The origin of the first metacarpal coordinate system was midway of the *Y*-axis. The *X*-axis was defined as the axis forming a sagittal plane that splits the first metacarpal into mirror images with the *Y*-axis, and the *Z*-axis was the common line perpendicular to the *X*- and *Y*-axes. The cartilage region was segmented in the cartilage + bone model, and the border of the articular surface was manually selected by carefully tracing the visible perimeter of the cartilage and referring to the subchondral bone surface of the bone model[4,9,20–22]. This ROI of the entire cartilaginous surface was named *TOTAL*. Finally, this region was quadrisected in the dorsal-to-volar direction by planes parallel to the *Y*–*Z* plane (coronal plane). The ROIs located in the dorsal, central-dorsal, central-volar, and volar sides were named *D*, *CD*, *CV*, and *V*, respectively (Fig. 2).

In the trapezium, we similarly used an ISB orthogonal coordinate system[23,24]. The *y*-axis extended from the exact mid-point of the central ridge of the trapezial saddle to the center of the junction of the trapezium, scaphoid, and trapezoid (the mid-point was the origin of the trapezial coordinate system). The *x*-axis ran in the dorsal-to-volar direction along a line perpendicular to the central ridge of the trapezium and passed through the mid-point of the dorsal surface to the proximal volar pole of the tubercle of the trapezium. The *z*-axis was perpendicular to the *x*- and *y*-axes and nearly parallel to the central ridge of the articular surface. Similar to the first metacarpal counterpart, the cartilage region, named *total*, was manually segmented and quadrisected in the dorsal-to-volar direction by planes parallel to the *y*–*z* plane (coronal plane). Additionally, the ROIs located in the dorsal, central-dorsal, central-volar, and volar sides were named *d*, *cd*, *cv*, and *v*, respectively (Fig. 2).

Cartilage thickness evaluation

We imported the STL data of the ROIs into Geomagic Control software and measured the average cartilage thickness value for each ROI (*D*, *CD*, *CV*, *V*, and *TOTAL* in the first metacarpal and *d*, *cd*,

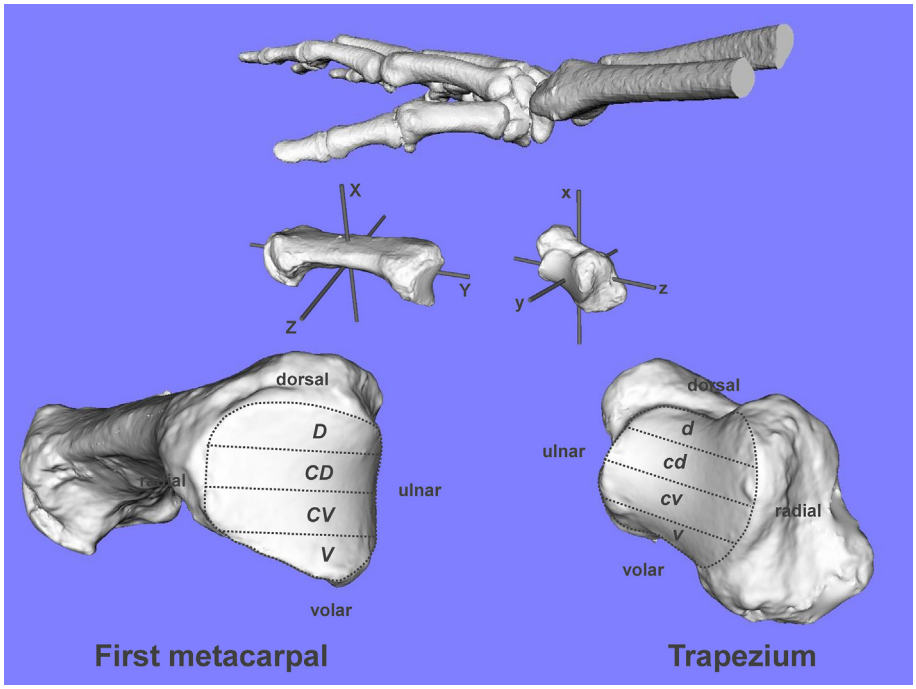

Fig. 2. Definitions of the regions of interest (ROIs). On the articular surfaces of the first metacarpal (left) and trapezium (right), the ROIs are defined in the dorsal-to-volar direction as *D*, *CD*, *CV*, and *V*, and as *d*, *cd*, *cv*, and *v*, respectively (see the text for the definition of each coordinate axis).

cv, *v*, and *total* in the trapezium). The thickness was measured for all points sampled on the articular surface by ascertaining the minimum spatial distance between the cartilage + bone and bone models, and the cartilage thickness was obtained by averaging the values of all points in a categorized region. The mean numbers of points sampled within the articular surface were 33,911 ± 7,062 for the first metacarpal and 35,169 ± 7,667 for the trapezium.

Radiographic evaluation

Based on the acquired CT data of specimens, we generated digitally reconstructed radiographs of the TMC joint of the hand (posteroanterior [PA] view) using a DICOM viewer (Synapse Vincent; Fuji Film, Tokyo, Japan) to assess the radiographic severity according to the Eaton–Glickel classification (Fig. 3)[25–27]. We defined the hand PA view so that the third metacarpophalangeal joint was at the center[27,28]. Each TMC joint was graded for overall radiographic OA using the Eaton classification system[27] (1 = slight widening of the TMC joint space and normal articular contours; 2 = mild narrowing of the TMC joint space, spurs or debris < 2 mm along the joint margins, and early erosion of the dorsal radial facet of the trapezium; 3 = marked narrowing of the TMC joint space, debris > 2 mm, and cystic and sclerotic changes in the subchondral bone; and 4 = marked narrowing or destruction of the surfaces of both the TMC joint and scaphotrapezial joint. Reportedly, this stage involves multiple articular surfaces).

Statistical analysis

In this study, all statistical analyses were performed using IBM SPSS, version 23.0 (IBM Corp., Armonk, NY, USA), and the significance level was set at $P < 0.05$. We tested the normality of all variables in the analyses using Shapiro–Wilk parametric tests, and measurements of all groups/subgroups exhibited a normal distribution. Hence, we used parametric models in the statistical analyses in this study.

To detect differences in the cartilage thickness among *D*, *CD*, *CV*, and *V* in the first metacarpal and *d*, *cd*, *cv*, and *v* in the trapezium, data were analyzed using one-way analysis of variance and unpaired *t*-tests with Bonferroni adjustment for multiple comparisons.

Correlations of cartilage thickness measurements with age and sex were investigated using Pearson correlation coefficients (r) for each ROI. The strength of correlation was classified as slight ($r < 0.2$), low ($r = 0.2–0.4$), moderate ($r = 0.4–0.7$), or high ($r > 0.7$)[29].

Before the analyses, interobserver reproducibility of three authors (S.M., R.S., and H.T.) for Eaton grade scoring was assessed using the intraclass correlation coefficient (ICC). Subsequently, we compared the Eaton grades with cartilage measurements for each ROI using r to assess the correlations between region-specific cartilage thickness patterns and radiographic severity.

Priori power analyses (adjusted alpha = 0.05/4 = 0.0125, beta = 0.2, two-tailed) were conducted to detect a cartilage thickness difference of 0.15 ± 0.12 mm[10]. In analyses of both the first metacarpal and trapezium, the minimum sample size to identify meaningful differences was 16 specimens.

Results

The cartilage wear patterns were represented as 3-D thickness maps of the first metacarpal and trapezium from typical subjects (Fig. 4). Figures 5A and 5B show the distributions of the cartilage thickness measurements of the first metacarpal and trapezium. In the first metacarpal, the cartilage thickness tended to decline volarly (the mean cartilage thickness of *V* was 0.32 ± 0.16 mm, whereas that of *D* was 0.53 ± 0.18 mm). Statistically significant differences were noted between the following regions: *D* vs *CV*, *D* vs *V*, *CD* vs *CV*, and *CD* vs *V* (Table IA). Conversely, the cartilage in the trapezium was evenly distributed in the dorsal-to-volar direction on the articular surface (the mean cartilage thickness values of *d*, *cd*, *cv*, and *v* were 0.46 ± 0.18 mm, 0.37 ± 0.17 mm, 0.35 ± 0.19 mm, and

Fig. 3. Digitally reconstructed radiographs. The trapeziometacarpal (TMC) joint is graded in the hand posteroanterior (PA) view.

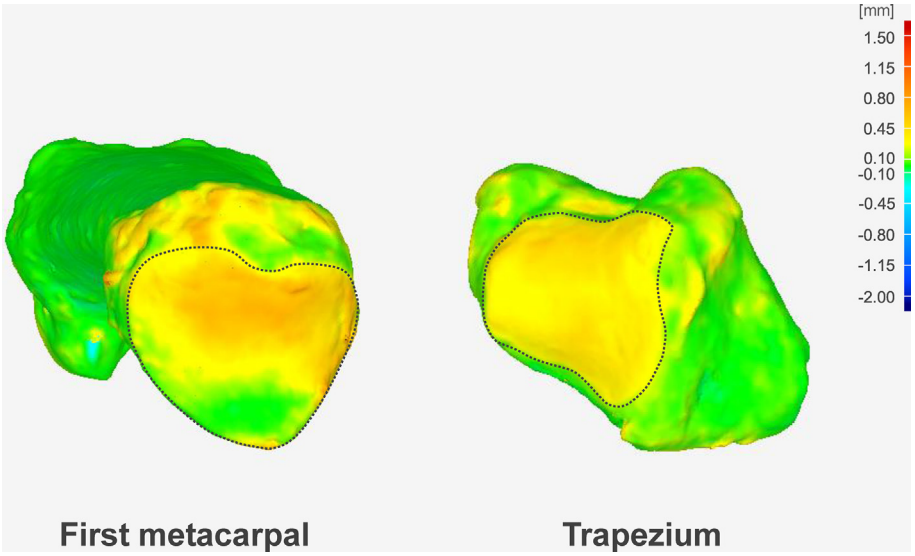

Fig. 4. Three-dimensional cartilage distribution patterns of the first metacarpal (left) and trapezium (right).

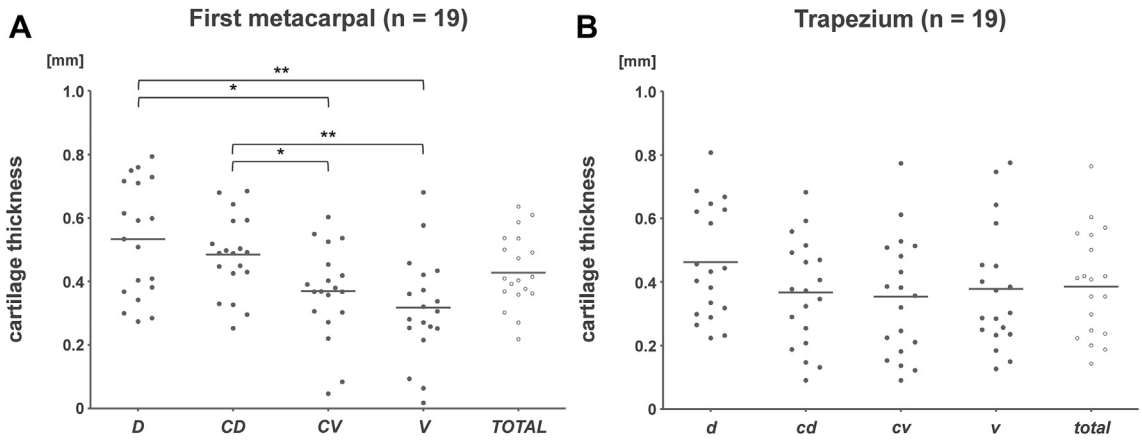

Fig. 5. Cartilage thickness distributions for the first metacarpal (A) and trapezium (B). Results are shown for divided ROIs (filled circle) and their total (open circle). Abscissa, cartilage thickness (mm); ordinate, ROIs. Asterisks indicate statistically significant differences (*$P < 0.05$ and **$P < 0.01$). SD, standard deviation; IQR, interquartile range.

Table IA
Comparison of the first metacarpal cartilage thickness among *D, CD, CV, and V* [mm]

	ROI data					*P*-value	*P*-value with Bonferroni adjustment					
	D	*CD*	*CV*	*V*	*TOTAL*	One-way ANOVA	*D* vs *CD*	*D* vs *CV*	*D* vs *V*	*CD* vs *CV*	*CD* vs *V*	*CV* vs *V*
Mean ± SD	0.53 ± 0.18	0.48 ± 0.12	0.37 ± 0.14	0.32 ± 0.16	0.43 ± 0.11	**< 0.001**	>0.999	**0.016**	**< 0.001**	**0.048**	**0.004**	>0.999
Median [IQR]	0.54 [0.38, 0.72]	0.49 [0.43, 0.56]	0.37 [0.31, 0.44]	0.31 [0.26, 0.40]	0.40 [0.36, 0.51]							
Range	0.28–0.80	0.26–0.69	0.05–0.61	0.02–0.68	0.21–0.63							

SD, standard deviation; IQR, interquartile range; ANOVA, analysis of variance.
Statistically significant *P*-values ($P < 0.05$) are indicated in bold.

0.38 ± 0.19 mm, respectively. However, we did not detect any statistical differences among the ROIs (Table IB).

Cartilage measurements showed high-to-moderate correlations with age in *CD*, *CV*, *V*, and *TOTAL* of the first metacarpal ($r = -0.53$ to -0.78) and in all ROIs of the trapezium ($r = -0.58$ to -0.75) [Fig. 6(A)]. Additionally, the measurements showed moderate correlations with sex in *CV* and *V* of the first metacarpal ($r = -0.54$ and -0.61, respectively) and in *cd*, *cv*, *v*, and *total* of the trapezium ($r = -0.50$ to -0.52) [Fig. 6(B)].

All specimens were radiographically categorized according to the Eaton grade as follows: Eaton grade 1, zerojoints; Eaton grade 2, five joints; Eaton grade 3, eight joints; and Eaton grade 4, six joints. The ICC of Eaton grade scoring was 0.87 for interobserver reproducibility. In no specimen, all three observers provided a different grade, and Eaton grades matching for at least two observers were used in the analysis. Figure 7 presents the correlations of the Eaton grades with cartilage measurements for the different ROIs. In the first metacarpal, cartilage measurements showed high-to-moderate correlations with the Eaton grades in *CV* and *V* ($r = -0.70$ and -0.48, respectively) and low correlations with the Eaton grades in *D*, *CD*, and *TOTAL* ($r = 0.29$, -0.22, and -0.34, respectively). On the other hand, in the trapezium, cartilage

Table IB
Comparison of the trapezial cartilage thickness among *d, cd, cv, and v* [mm]

	ROI data					*P*-value	*P*-value with Bonferroni adjustment					
	d	*cd*	*cv*	*v*	*total*	One-way ANOVA	*d* vs *cd*	*d* vs *cv*	*d* vs *v*	*cd* vs *cv*	*cd* vs *v*	*cv* vs *v*
Mean ± SD	0.46 ± 0.18	0.37 ± 0.17	0.35 ± 0.19	0.38 ± 0.19	0.39 ± 0.17	0.375	0.392	0.304	0.68	>0.999	>0.999	>0.999
Median [IQR]	0.44 [0.31, 0.63]	0.38 [0.23, 0.48]	0.36 [0.20, 0.50]	0.31 [0.25, 0.46]	0.40 [0.24, 0.52]							
Range	0.23–0.81	0.09–0.69	0.09–0.78	0.13–0.78	0.14–0.76							

SD, standard deviation; IQR, interquartile range; ANOVA, analysis of variance.

measurements showed high-to-moderate correlations with the Eaton grades in *cd*, *cv*, *v*, and *total* ($r = -0.59$ to -0.72).

Discussion

In this study, we created 3-D cartilage models from cadaveric TMC joints using a laser scanner and quantitatively analyzed the cartilage wear pattern in severe OA cases. The findings of the first metacarpal revealed that greater disease stage is associated with more severe cartilage wear on the volar side, whereas the findings of the trapezium interestingly revealed that the cartilage evenly degenerated throughout the articular surface in the late disease stage. Particularly, cartilage measurements showed good correlations with age and sex in the regions where cartilage thinning was remarkable. Furthermore, we investigated the correlations between cartilage thickness measurements and OA severity according to the Eaton grading system. Correlation analyses revealed good correlations between radiographic staging and cartilage measurements in these regions as well.

A challenge in quantifying the cartilage wear of the TMC joint, particularly in the advanced OA stage, arises because of its thinness, its shape complexity, and the spatial variability of its worn-out pattern. Until now, few anatomical studies focused on the cartilage thickness of the TMC joint. Koff *et al.* reported that the mean cartilage thicknesses of the first metacarpal and trapezium under normal conditions were approximately 0.7 and 0.8 mm, respectively[10]. In addition, there is consensus that cartilage degeneration of the first metacarpal originates and progresses from the volar area[4,10,30–32]. On the other hand, cartilage thinning in the trapezium is considered to volarly expand; however, this contradicts our findings[4,10,31]. These patterns were identified to have close relations to high load bearing in previous contact area studies[9,22,33–40]. With regard to age- and sex-related associations, our correlation analyses supported the trends of cartilage wear pattern in both the first metacarpal and trapezium, although Halilaj *et al.* reported that cartilage thickness does not differ according to age and sex in normal or early OA subjects[41]. Efforts have been focused on the radiographic detection of this cartilage degeneration, and the Eaton classification was developed and validated on the basis of treatment follow-up results of OA cases[27,32,42]. Particularly, radiographic staging is considered more sensitive to detect advanced-stage OA[10]. To the best of our knowledge, to date, only few studies have investigated the 3-D cartilage wear patterns during late OA of the TMC joint[4,9,10], further associating with the radiographic classification. Hence, this study adds relevant information to the findings of previous anatomical studies in these aspects.

The results of the first metacarpal revealed that the cartilage tended to be thinner at the volar region of the articular surface, which is almost similar to the findings reported in previous studies[4,10,30–32]. This was supported by evidence indicating that the greatest contact occurs on the volar surface with daily activities, which provided a theory that abnormally high stresses, such as so-called “screw-home torque,” might initiate or exacerbate OA progression in the articular cartilage[9,10,22,33–40]. Furthermore, measurements showed high-to-moderate correlations with Eaton grades in the region of the volar aspect where the cartilage thickness was markedly lower, and this supported our cartilage finding of a volar-dominant wear pattern in the advanced OA stage. Conversely, the cartilage of the trapezium was evenly thin across the entire articular surface, and measurements showed high-to-moderate correlations with Eaton grades. With regard to the trapezial cartilage wear pattern, the findings were not completely consistent with those of previous studies suggesting that cartilage degeneration progresses in the volar portion[4,10,31]. This could be primarily attributed to the fact that our subjects were in the advanced stage of OA, and osteophyte formation, morphological changes of the bones, and soft tissue contracture among individuals in the advanced stage might contribute to cartilage wear by augmenting joint incongruity and altering contact loading. Additionally, some findings with regard to our cartilage measurements, such as good correlations with age and sex and even distributions on the first metacarpal and trapezial articular surfaces in the radial-to-ulnar direction, were not consistent with the results in previous reports[4,10,31,41]. This might also be explained by the characteristics of the study population. Overall, the volar region of the cartilage of the first metacarpal could become articulate with the entire cartilaginous surface of the trapezium within the subluxated joints as the disease progresses; thus, cartilage wear patterns varied between the first metacarpal and trapezium in our advanced OA specimens. This might explain why cartilaginous and bony degradations of the first metacarpal show patterns that differ from those of the trapezium in advanced OA stages[4,9,10,21].

The present study had several strengths. First, we analyzed the 3-D cartilage wear patterns with a focus on the advanced stage of degeneration. Elucidating regional variation in cartilage loss is essential for ascertaining the articular cartilage wear pattern of the TMC joint, and it enables the illustration of the etiology of TMC OA. In addition, our findings were clinically relevant with regard to the treatment options for advanced OA. The leading surgical options for advanced-stage OA include complete or partial trapeziectomy, which are often applied in combination with arthroscopic intervention, ligament reconstruction, or interposition suspensionplasty[43]. Furthermore, the findings of this study could be useful in arthroscopic procedures, and the findings of the residual first metacarpal cartilage would help to realign the joint or reconstruct the ligament.

Conversely, the present study had several potential limitations. First, we only included specimens from elderly subjects, and there were no comparisons with normal control data from young and healthy specimens. However, only subjects with advanced-stage OA were included; hence, our findings can be considered representative of patients with advanced disease. Additionally, we consider our measurements of worn-out cartilage as reasonable when referring to previous results that indicated a normal cartilage thickness of 0.7–0.8 mm[10]. Hence, our findings add highly relevant information to existing data. Second, we used cadavers fixed in

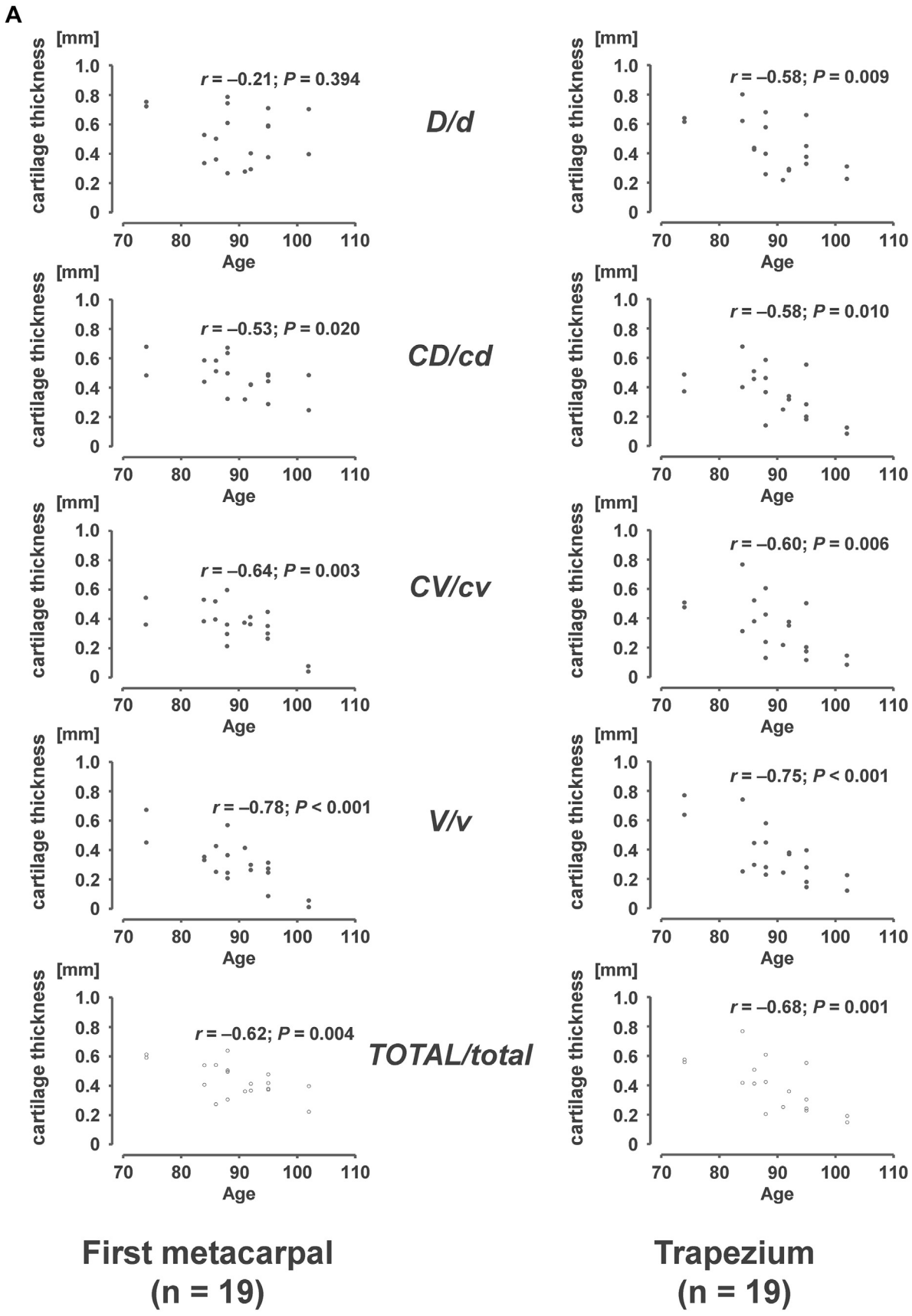

Fig. 6. Correlations of the cartilage thickness with age (A) and sex (B) for the first metacarpal (left) and trapezium (right). Results are shown for divided ROI (filled circle) and their total (open circle). Abscissa, cartilage thickness (mm); ordinate, age or sex.

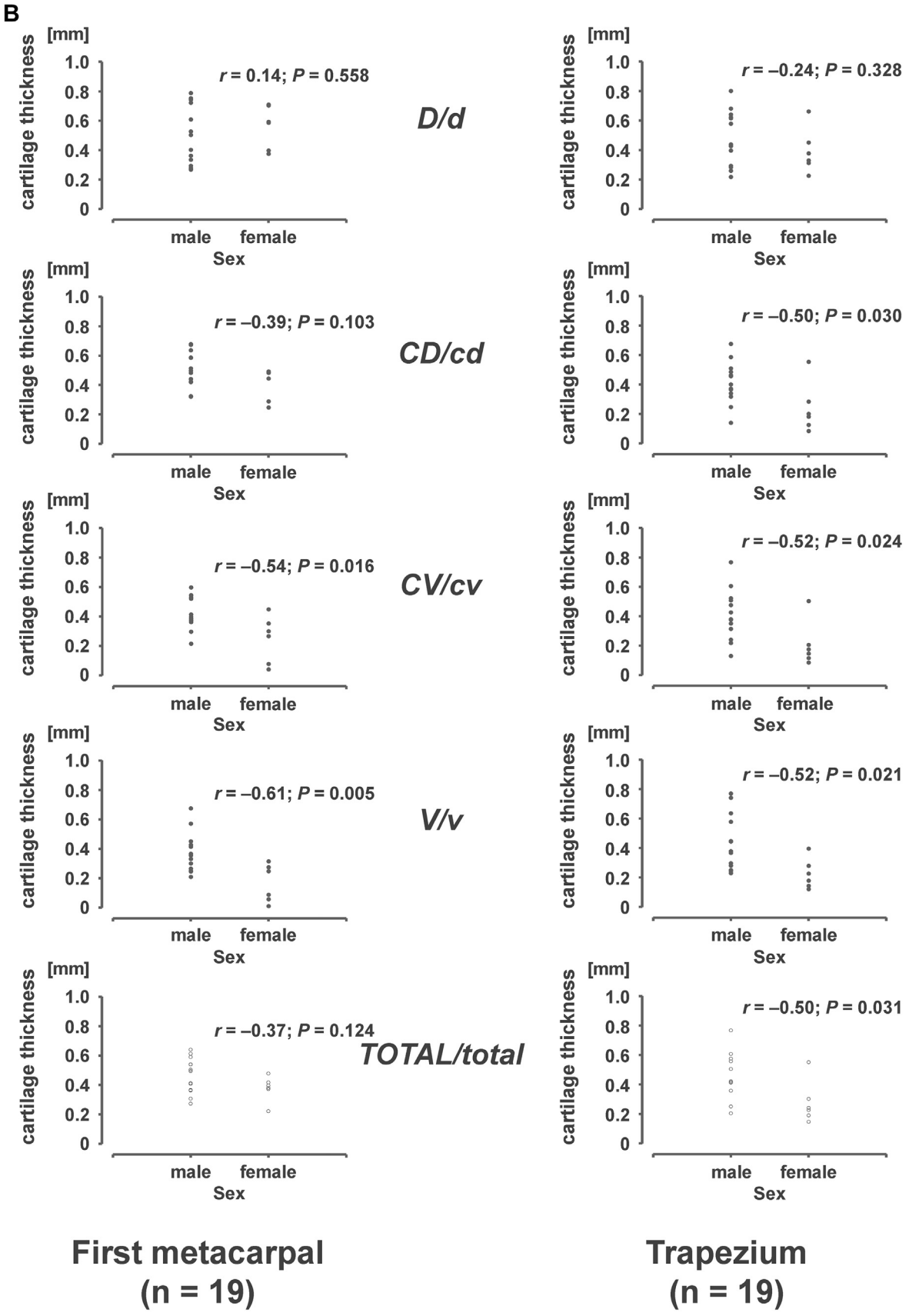

Fig. 6. (*continued*).

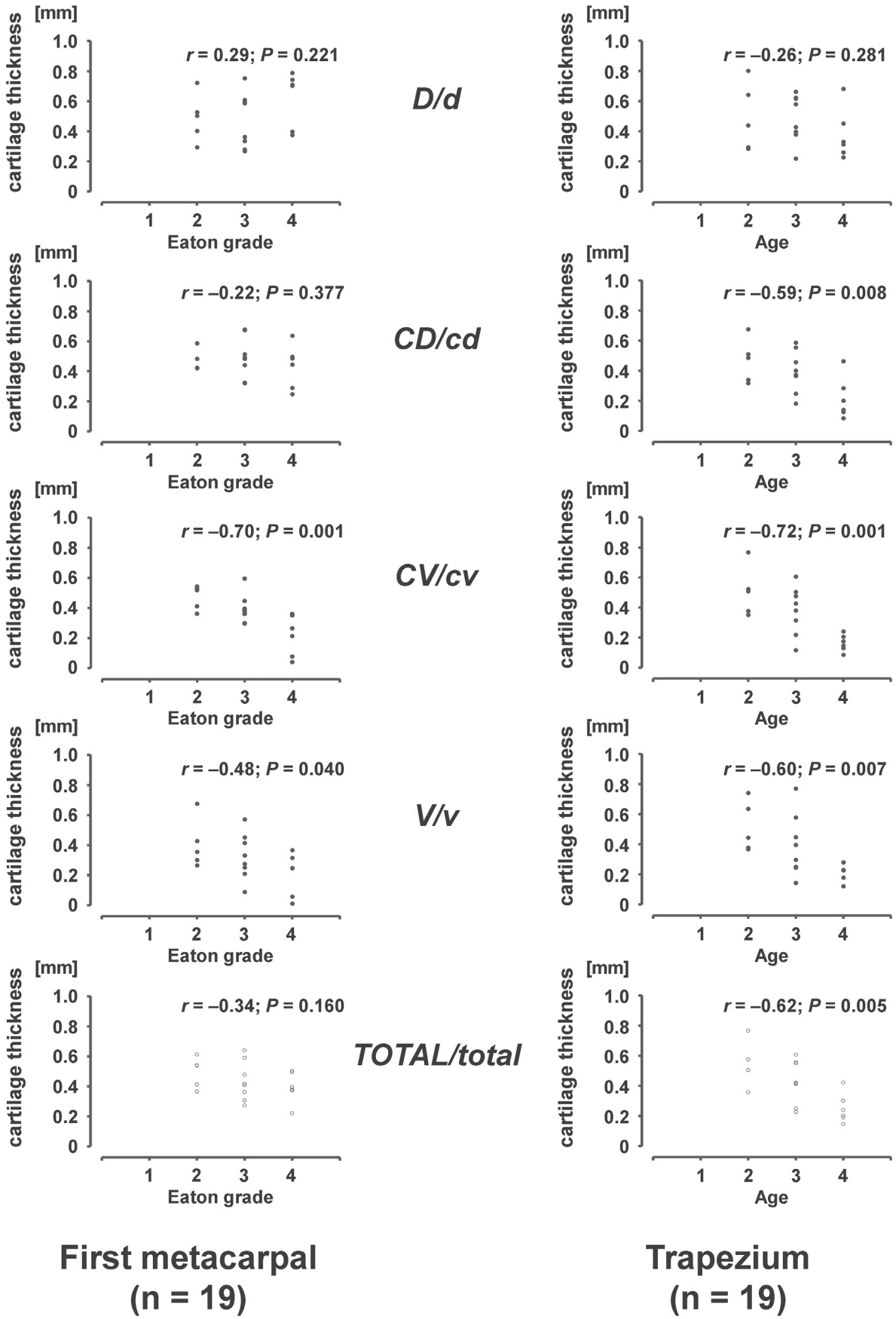

Fig. 7. Correlations between the cartilage thickness and the Eaton grade for the first metacarpal (left) and trapezium (right). Results are shown for divided ROI (filled circle) and their total (open circle). Abscissa, cartilage thickness (mm); ordinate, Eaton grade.

formalin. However, several studies have reported that formalin fixation has no measurable effect on the cartilage thickness or geometric configuration within joints[44–46]. Third, our study subjects were sampled without considering potential differences in age and sex. Correlation analyses supported the study results; however, a true correlation might have been overlooked or overestimated. Fourth, our sample size was insufficiently large, and the study was designed assuming a large effect size. Hence, a true difference might have been overlooked. Finally, no clinical data were obtained. As an illustration, considering the close association between cartilage wear patterns and age in the present study, cartilage wear might not progress as much in young OA patients; however, we often encounter young patients with pain related to TMC OA in the clinical setting. Thus, cartilage wear might not always represent clinical symptoms. For conclusive data, further studies are warranted to overcome these limitations and enhance the generalizability of the findings.

Conclusions

We identified regional variations in the cartilage wear patterns of the first metacarpal and trapezium during different OA stages by analyzing 3-D laser-scanned models, and our findings were supported by correlations with the Eaton grading system. A greater disease stage is associated with more severe wear at the volar region of the cartilage in the first metacarpal, whereas the cartilage is evenly degenerated throughout the articular surface in the trapezium, which can be considered novel and unprecedented observations. These findings provide additional insights for the elucidation of the etiology of TMC OA.

Author contributions

All authors contributed to the conception and design of the study, all were involved in drafting the article critically for important intellectual content, and all approved the content of the manuscript. Tsuyoshi Murase (E-mail: tmurase-osk@umin.ac.jp) had full access to all data in the study and takes responsibility for the integrity of the data and the accuracy of the data analysis. Specific roles were as follows. Study conception and design: Satoshi Miyamura, Takashi Sakai, Kunihiro Oka, Ryoya Shiode, Hiroyuki Tanaka, Tatsuo Mae, Kazuomi Sugamoto, Hideki Yoshikawa, and Tsuyoshi Murase. Acquisition of data: Satoshi Miyamura, Kunihiro Oka, and Tsuyoshi Murase. Analysis and interpretation of data: Satoshi Miyamura, Takashi Sakai, Kunihiro Oka, Ryoya Shiode, Hiroyuki Tanaka, Tatsuo Mae, Kazuomi Sugamoto, Hideki Yoshikawa, and Tsuyoshi Murase.

Competing interest statement

The authors certify that no commercial associations are present that might pose a conflict of interest in this paper.

Role of the funding source

This study was supported, in part, by a grant from Japan Agency for Medical Research and Development (Project ID 15570777) and by Japan Society for the Promotion of Science KAKENHI (Grant Number JP 15K10442).

Acknowledgments

We thank Ryoji Nakao and Taro Adachi for skillful technical support and their excellent contributions to this study.

Supplementary data

Supplementary data to this article can be found online at https://doi.org/10.1016/j.joca.2019.03.006.

References

1. Williams A, Shetty SK, Burstein D, Day CS, McKenzie C. Delayed gadolinium enhanced MRI of cartilage (dGEMRIC) of the first carpometacarpal (1CMC) joint: a feasibility study. Osteoarthritis Cartilage 2008;16:530–2.
2. Sodha S, Ring D, Zurakowski D, Jupiter JB. Prevalence of osteoarthrosis of the trapeziometacarpal joint. J Bone Jt Surg Am 2005;87:2614–8.
3. Rivers PA, Rosenwasser MP, Mow VC, Pawluk RJ, Strauch RJ, Sugalski MT, *et al*. Osteoarthritic changes in the biochemical composition of thumb carpometacarpal joint cartilage and correlation with biomechanical properties. J Hand Surg Am 2000;25:889–98.
4. Dourthe B, Nickmanesh R, Wilson DR, D'Agostino P, Patwa AN, Grinstaff MW, *et al*. Assessment of healthy trapeziometacarpal cartilage properties using indentation testing and contrast-enhanced computed tomography. Clin Biomech (Bristol, Avon) 2019;61:181–9.
5. Saltzherr MS, Coert JH, Selles RW, van Neck JW, Jaquet JB, van Osch GJ, *et al*. Accuracy of magnetic resonance imaging to detect cartilage loss in severe osteoarthritis of the first carpometacarpal joint: comparison with histological evaluation. Arthritis Res Ther 2017;19:55.
6. Dieppe PA, Lohmander LS. Pathogenesis and management of pain in osteoarthritis. Lancet 2005;365:965–73.
7. Sowers MF, Hayes C, Jamadar D, Capul D, Lachance L, Jannausch M, *et al*. Magnetic resonance-detected subchondral bone marrow and cartilage defect characteristics associated with pain and X-ray-defined knee osteoarthritis. Osteoarthritis Cartilage 2003;11:387–93.
8. Andriacchi TP, Koo S, Scanlan SF. Gait mechanics influence healthy cartilage morphology and osteoarthritis of the knee. J Bone Jt Surg Am 2009;91(Suppl 1):95–101.
9. Dourthe B, D'Agostino P, Stockmans F, Kerkhof F, Vereecke E. In vivo contact biomechanics in the trapeziometacarpal joint using finite deformation biphasic theory and mathematical modelling. Med Eng Phys 2016;38:108–14.
10. Koff MF, Ugwonali OF, Strauch RJ, Rosenwasser MP, Ateshian GA, Mow VC. Sequential wear patterns of the articular cartilage of the thumb carpometacarpal joint in osteoarthritis. J Hand Surg Am 2003;28:597–604.
11. Hadler NM, Gillings DB, Imbus HR, Levitin PM, Makuc D, Utsinger PD, *et al*. Hand structure and function in an industrial setting. Arthritis Rheum 1978;21:210–20.
12. Hunter DJ, Zhang Y, Sokolove J, Niu J, Aliabadi P, Felson DT. Trapeziometacarpal subluxation predisposes to incident trapeziometacarpal osteoarthritis (OA): the Framingham Study. Osteoarthritis Cartilage 2005;13:953–7.
13. Bowers ME, Trinh N, Tung GA, Crisco JJ, Kimia BB, Fleming BC. Quantitative MR imaging using "LiveWire" to measure tibiofemoral articular cartilage thickness. Osteoarthritis Cartilage 2008;16:1167–73.
14. Bullough PG, Jagannath A. The morphology of the calcification front in articular cartilage. Its significance in joint function. J Bone Jt Surg Br 1983;65:72–8.
15. Koo S, Gold GE, Andriacchi TP. Considerations in measuring cartilage thickness using MRI: factors influencing reproducibility and accuracy. Osteoarthritis Cartilage 2005;13:782–9.
16. Millington SA, Grabner M, Wozelka R, Anderson DD, Hurwitz SR, Crandall JR. Quantification of ankle articular cartilage topography and thickness using a high resolution stereophotography system. Osteoarthritis Cartilage 2007;15:205–11.

17. Podolsky D, Mainprize J, McMillan C, Binhammer P. Comparison of third toe joint cartilage thickness to that of the finger proximal interphalangeal (PIP) joint to determine suitability for transplantation in PIP joint reconstruction. J Hand Surg Am 2011;36:1950–8.
18. Besl P, McKay N. A method for registration of 3D shapes. IEEE Trans Patt Anal 1992;14:239–56.
19. Wu G, van der Helm FC, Veeger HE, Makhsous M, Van Roy P, Anglin C, *et al*. ISB recommendation on definitions of joint coordinate systems of various joints for the reporting of human joint motion–Part II: shoulder, elbow, wrist and hand. J Biomech 2005;38:981–92.
20. Halilaj E, Rainbow MJ, Got CJ, Moore DC, Crisco JJ. A thumb carpometacarpal joint coordinate system based on articular surface geometry. J Biomech 2013;46:1031–4.
21. D'Agostino P, Dourthe B, Kerkhof F, Harry Van Lenthe G, Stockmans F, Vereecke EE. In vivo biomechanical behavior of the trapeziometacarpal joint in healthy and osteoarthritic subjects. Clin Biomech (Bristol, Avon) 2017;49:119–27.
22. Halilaj E, Moore DC, Patel TK, Laidlaw DH, Ladd AL, Weiss AP, *et al*. Older asymptomatic women exhibit patterns of thumb carpometacarpal joint space narrowing that precede changes associated with early osteoarthritis. J Biomech 2015;48:3634–40.
23. Cooney 3rd WP, Lucca MJ, Chao EY, Linscheid RL. The kinesiology of the thumb trapeziometacarpal joint. J Bone Jt Surg Am 1981;63:1371–81.
24. Xu L, Strauch RJ, Ateshian GA, Pawluk RJ, Mow VC, Rosenwasser MP. Topography of the osteoarthritic thumb carpometacarpal joint and its variations with regard to gender, age, site, and osteoarthritic stage. J Hand Surg Am 1998;23:454–64.
25. Altman RD, Gold GE. Atlas of individual radiographic features in osteoarthritis, revised. Osteoarthritis Cartilage 2007;15(Suppl A):A1–A56.
26. Chaisson CE, Zhang Y, McAlindon TE, Hannan MT, Aliabadi P, Naimark A, *et al*. Radiographic hand osteoarthritis: incidence, patterns, and influence of pre-existing disease in a population based sample. J Rheumatol 1997;24:1337–43.
27. Eaton RG, Glickel SZ. Trapeziometacarpal osteoarthritis. Staging as a rationale for treatment. Hand Clin 1987;3:455–71.
28. Riordan E, Robbins S, Deveza L, Duong V, Oo WM, Wajon A, *et al*. Radial subluxation in relation to hand strength and radiographic severity in trapeziometacarpal osteoarthritis. Osteoarthritis Cartilage 2018;26:1506–10.
29. Guilford JP. Fundamental Statistics in Psychology and Education. 3rd edn. New York: McGraw-Hill Book Company; 1956.
30. Doerschuk SH, Hicks DG, Chinchilli VM, Pellegrini Jr VD. Histopathology of the palmar beak ligament in trapeziometacarpal osteoarthritis. J Hand Surg Am 1999;24:496–504.
31. Eaton RG, Lane LB, Littler JW, Keyser JJ. Ligament reconstruction for the painful thumb carpometacarpal joint: a long-term assessment. J Hand Surg Am 1984;9:692–9.
32. Eaton RG, Littler JW. Ligament reconstruction for the painful thumb carpometacarpal joint. J Bone Jt Surg Am 1973;55:1655–66.
33. North ER, Rutledge WM. The trapezium-thumb metacarpal joint: the relationship of joint shape and degenerative joint disease. Hand 1983;15:201–6.
34. Pellegrini Jr VD, Olcott CW, Hollenberg G. Contact patterns in the trapeziometacarpal joint: the role of the palmar beak ligament. J Hand Surg Am 1993;18:238–44.
35. Ateshian GA, Ark JW, Rosenwasser MP, Pawluk RJ, Soslowsky LJ, Mow VC. Contact areas in the thumb carpometacarpal joint. J Orthop Res 1995;13:450–8.
36. D'Agostino P, Dourthe B, Kerkhof F, Stockmans F, Vereecke EE. In vivo kinematics of the thumb during flexion and adduction motion: evidence for a screw-home mechanism. J Orthop Res 2017;35:1556–64.
37. Edmunds JO. Traumatic dislocations and instability of the trapeziometacarpal joint of the thumb. Hand Clin 2006;22:365–92.
38. Edmunds JO. Current concepts of the anatomy of the thumb trapeziometacarpal joint. J Hand Surg Am 2011;36:170–82.
39. Goto A, Leng S, Sugamoto K, Cooney 3rd WP, Kakar S, Zhao K. In vivo pilot study evaluating the thumb carpometacarpal joint during circumduction. Clin Orthop Relat Res 2014;472:1106–13.
40. Kawanishi Y, Oka K, Tanaka H, Okada K, Sugamoto K, Murase T. In vivo 3-dimensional kinematics of thumb carpometacarpal joint during thumb opposition. J Hand Surg Am 2018;43:182.e1–7.
41. Halilaj E, Laidlaw DH, Moore DC, Crisco JJ. How Do Sex, Age, and Osteoarthritis Affect Cartilage Thickness at the Thumb Carpometacarpal Joint? Insights from Subject-specific Cartilage Modeling. Cham, Switzerland: Springer International Publishing; 2014, 103–11.
42. Eaton RG, Littler JW. A study of the basal joint of the thumb. Treatment of its disabilities by fusion. J Bone Jt Surg Am 1969;51:661–8.
43. Van Heest AE, Kallemeier P. Thumb carpal metacarpal arthritis. J Am Acad Orthop Surg 2008;16:140–51.
44. Adam C, Eckstein F, Milz S, Schulte E, Becker C, Putz R. The distribution of cartilage thickness in the knee-joints of old-aged individuals – measurement by A-mode ultrasound. Clin Biomech (Bristol, Avon) 1998;13:1–10.
45. Akiyama K, Sakai T, Koyanagi J, Yoshikawa H, Sugamoto K. Morphological analysis of the acetabular cartilage surface in elderly subjects. Surg Radiol Anat 2015;37:963–8.
46. Kurrat HJ, Oberlander W. The thickness of the cartilage in the hip joint. J Anat 1978;126:145–55.